ARTICLE

Self-Assembled Graphene Hydrogel *via* a One-Step Hydrothermal Process

Yuxi Xu, Kaixuan Sheng, Chun Li, and Gaoquan Shi*

Department of Chemistry, Tsinghua University, Beijing 100084, People's Republic of China

ABSTRACT Self-assembly of two-dimensional graphene sheets is an important strategy for producing macroscopic graphene architectures for practical applications, such as thin films and layered paperlike materials. However, construction of graphene self-assembled macrostructures with three-dimensional networks has never been realized. In this paper, we prepared a self-assembled graphene hydrogel (SGH) *via* a convenient one-step hydrothermal method. The SGH is electrically conductive, mechanically strong, and thermally stable and exhibits a high specific capacitance. The high-performance SGH with inherent biocompatibility of carbon materials is attractive in the fields of biotechnology and electrochemistry, such as drug-delivery, tissue scaffolds, bionic nanocomposites, and supercapacitors.

KEYWORDS: graphene · three-dimensional · self-assembly · hydrogel · hydrothermal reduction

Graphene has attracted intense interest all over the world in recent years, due to its single-atom thickness, flexible two-dimensional (2D) structure, and exceptional physical and chemical properties.[1−8] A great deal of work has shown the huge potential of graphene or chemically modified graphene in various technological fields, such as field-effect devices,[9,10] chemical and biological sensors,[11−13] energy-storage materials,[14−16] polymer composites,[17−19] and electrocatalysis.[20−22] It is well believed that graphene will play a central role in the coming era of nanotechnology.

Self-assembly has been recognized for a long time as one of the most effective strategies for "bottom-up" nanotechnology. With unique structure and properties, graphene naturally becomes a versatile nanoscale building block for self-assembly to achieve novel structures and functionalities. Recent work has successfully demonstrated the self-assembly of graphene sheets into high-performance thin films *via* multiple-step processes[23−32] such as transparent and conducting membranes[23−27] and strong layered paperlike materials.[28−32] However, self-assembling 2D graphene sheets into complex three-dimensional (3D) macrostructures remains to be realized for the purposes of further understanding their assembly behaviors and producing graphene-based materials with industrial interests. In this paper, we report a high-performance self-assembled graphene hydrogel (SGH) prepared by a facile one-step hydrothermal method. The SGH containing about 2.6% (by weight) graphene sheets and 97.4% water has an electrical conductivity as high as 5×10^{-3} S/cm. Furthermore, it is thermally stable in the temperature scale of 25−100 °C and its storage modulus (450−490 kPa) is about 1−3 orders of magnitude higher than those of conventional self-assembled hydrogels. The SGH as a 3D supercapacitor electrode material exhibits high specific capacitance (175 F/g) in an aqueous electrolyte.

RESULTS AND DISCCUSION

The typical SGH can be easily prepared by heating 2 mg/mL of homogeneous graphene oxide (GO) aqueous dispersion (Figure S1, Supporting Information) sealed in a Teflon-lined autoclave at 180 °C for 12 h (Figure 1a). The as-prepared SGH containing about 2.6 wt % of hydrothermally reduced GO (or graphene) and 97.4 wt % water is mechanically strong. Three SGH columns with a diameter around 0.8 cm each can support 100 g weight with little deformation (Figure 1b). This is very impressive since conventional self-assembled hydrogels reported previously are usually very weak.[33,34] The SGH has a well-defined and interconnected 3D porous network as imaged by scanning electron microscopy (SEM) of its freeze-dried samples (Figure 1c−e). The pore sizes of the network are in

*Address correspondence to gshi@tsinghua.edu.cn.

Received for review May 28, 2010 and accepted June 25, 2010.

Published online June 30, 2010. 10.1021/nn101187z

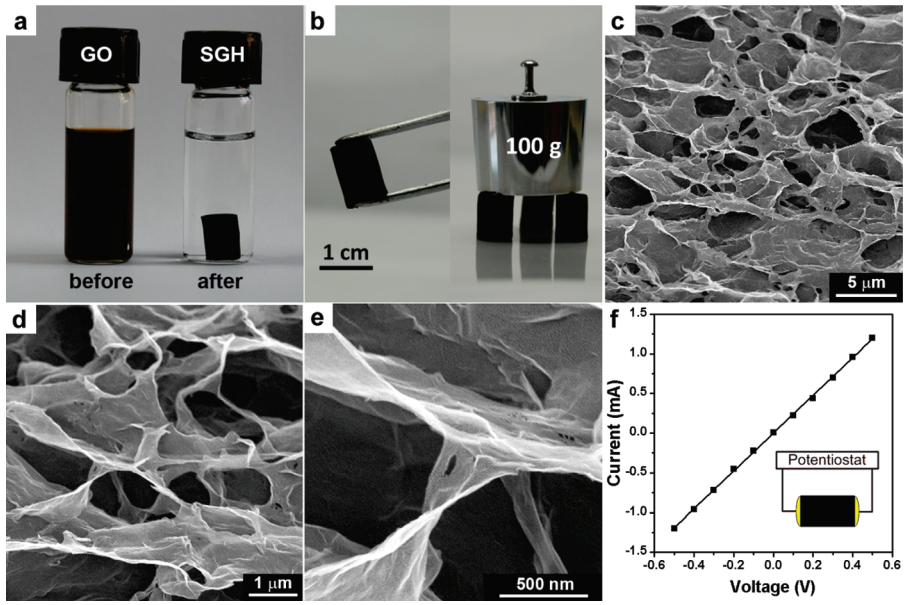

Figure 1. (a) Photographs of a 2 mg/mL homogeneous GO aqueous dispersion before and after hydrothermal reduction at 180 °C for 12 h; (b) photographs of a strong SGH allowing easy handling and supporting weight; (c−e) SEM images with different magnifications of the SGH interior microstructures; (f) room temperature *I*−*V* curve of the SGH exhibiting Ohmic characteristic, inset shows the two-probe method for the conductivity measurements.

the range of submicrometer to several micrometers and the pore walls consist of thin layers of stacked graphene sheets. The partial overlapping or coalescing of flexible graphene sheets resulted in the formation of physical cross-linking sites of the framework of the SGH (Figure 1e). Thus, the inherent flexibility of graphene sheets is a crucial property for constructing the 3D macrostructures.

In addition to the excellent apparent mechanical strength, the SGH is electrically conductive with a conductivity of about 5×10^{-3} S/cm (Figure 1f), which is also an attractive property for many practical applications.[35] This is mainly due to the recovery of π-conjugated system from GO sheets upon hydrothermal reduction, as confirmed by the X-ray diffraction (XRD) patterns shown in Figure 2. The interlayer spacing of the freeze-dried SGH was calculated to be 3.76 Å. This value is much lower than that of GO precursor (6.94 Å) while slightly higher than that of natural graphite (3.36 Å). These results suggest the existence of π−π stacking between graphene sheets in the SGH and also the presence of residual oxygenated functional groups on reduced GO sheets.[36] Thanks to these residual hydrophilic oxygenated groups (Supporting Information, Figure S2), the reduced GO sheets can encapsulate water in the process of self-assembly. This factor together with the π-stacking of graphene sheets resulted in the successful construction of the SGH. The broad XRD peak of the freeze-dried SGH indicates the poor ordering of graphene sheets along their stacking direction and reflects that the framework of the SGH is composed of few-layer stacked graphene sheets.

The structure and properties of the SGH were further studied by rheological tests. As shown in Figure 3a, the viscosity of the SGH diminished greatly as it was sheared, which is a typical characteristic of a self-assembled hydrogel with physical cross-links.[37] As described above, the formation of the SGH was driven by π−π stacking interactions of graphene sheets. During the shearing process, the noncovalent cross-links of the SGH were partly dissociated through the parallel sliding between graphene sheets, leading to the substantial decrease in viscosity of the SGH. Small-deformation oscillatory measurements revealed that the storage or elastic modulus (G') of the SGH is 1 order of magnitude higher than its loss or viscous modulus (G'') over the entire tested range of angular frequencies (1−100 rad/s, Figure 3b). This result implies that elastic response is predominant and the SGH has a permanent network. The G'' values of the SGH are slightly sensitive to angular frequency and do not cross over each other

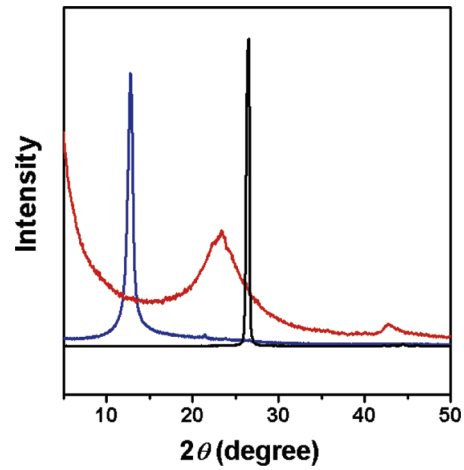

Figure 2. XRD patterns of natural graphite (black), GO (blue), and freeze-dried SGH (red).

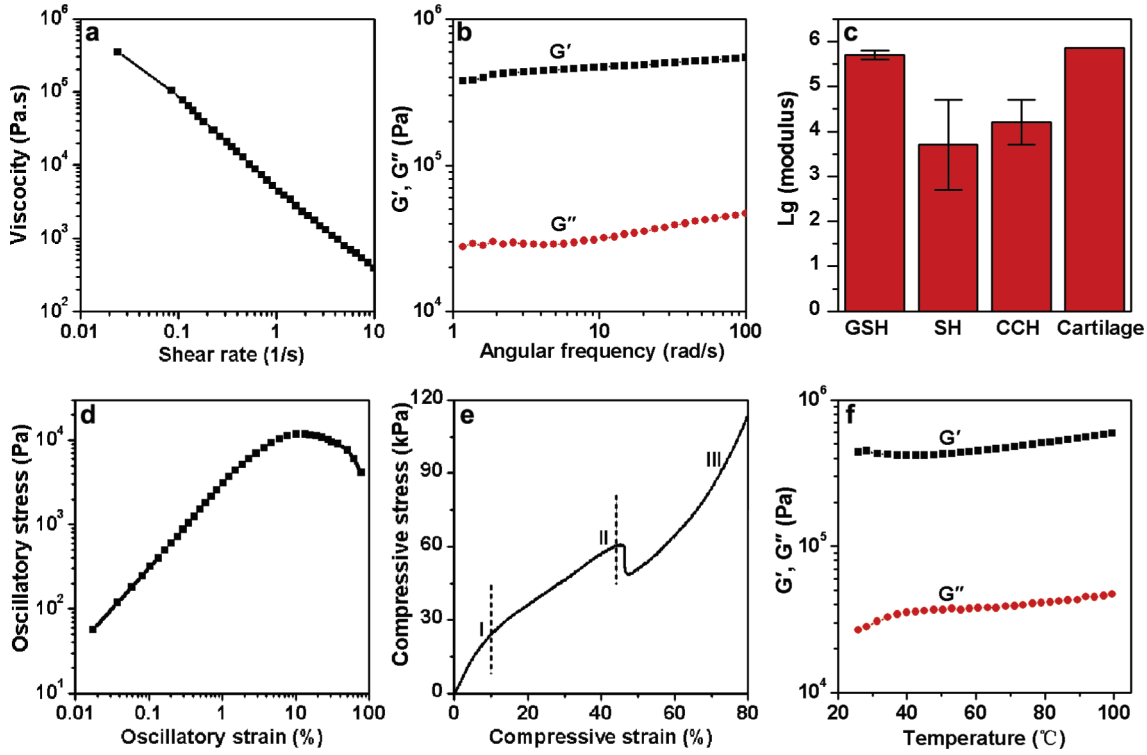

Figure 3. Steady (a) and dynamic (b) rheological behaviors of the SGH; (c) histogram for comparing the modulus of the SGH with those of typical self-assembled hydrogels (SHs), chemically cross-linked hydrogels (CCHs) and biological tissue cartilage reported in literature;[33−35] (d) oscillatory strain sweep curve of the SGH; (e) compressive stress−strain curve of the SGH; (f) storage (G') and loss (G'') moduli of the SGH as a function of temperature.

in the tested frequency range, which is a characteristic of gels with a high degree of covalent or noncovalent cross-linking. The G' of the SGH at 10 rad/s was measured to be about 470 kPa. This value is about 1−3 orders of magnitude higher than those of conventional self-assembled hydrogels that we have retrieved[33,34] and comparable to those of various chemically cross-linked polymer hydrogels and some biological tissues[35] (Figure 3c). An oscillatory strain sweep measurement was also taken to measure the yield stress (σ_c) of the SGH (Figure 3d). The stress of the SGH increases linearly with the strain amplitude applied to the sample in the initial stage; then it deviates from linearity at high strains. At the turning point, the stress reaches its maximum, and it is defined as σ_c. Above σ_c, the gel starts to flow and breaks. Thereby, apart from G', σ_c can also be used to assess the mechanical strength of the SGH. The σ_c of the SGH was measured to be about 11.7 kPa (Figure 3d), and this value is also much higher than those of other self-assembled hydrogels.[33,34] The extraordinary high mechanical strength of the SGH can be attributed to the excellent mechanical properties of graphene building blocks as well as its strong and dense cross-linking sites. The typical self-assembled hydrogels reported previously were usually constructed by self-assembling small molecules or macromolecules to form networks with physical cross-links. The driving forces for forming the physical cross-links are weak interactions, such as van der Waals force, hydrogen bonding, $\pi-\pi$ stacking, and inclusion interaction. In contrast, graphene sheet, the building block of the SGH, is one of the strongest materials ever found with a high Young's modulus (about 1.1 TPa) and fracture strength (about 125 GPa).[6] Moreover, the large conjugated structure of graphene sheets can provide them with many π-stacking sites to form extremely strong bindings be-

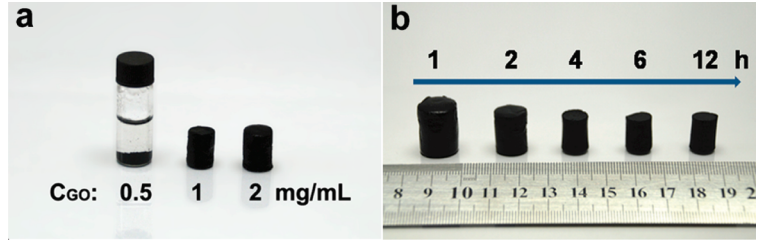

Figure 4. (a) Photographs of the products prepared by hydrothermal reduction of GO dispersions with different C_{GO} at 180 °C for 12 h; (b) photographs of the products prepared by hydrothermal reduction of 2 mg/mL of GO at 180 °C for different times.

TABLE 1. Summary of the Mechanical and Electrical Properties of the SGHs Prepared by Hydrothermal Reduction of 2 mg/mL GO for Different Times

SGHs (h)	C/O atomic ratio	Water content (wt %)	Storage modulus (kPa)	Oscillatory yield stress (kPa)	Compressive yield stress (kPa)	Compressive elastic modulus (kPa)	Electrical conductivity (mS/cm)
1	3.4	99.1 ± 0.1	55 ± 2	0.4 ± 0.02	3 ± 0.5	29 ± 3	0.23 ± 0.02
2	4.5	98.6 ± 0.1	260 ± 10	2.0 ± 0.1	9 ± 1	115 ± 10	1.2 ± 0.1
4	4.9	98.0 ± 0.1	395 ± 15	7.3 ± 0.3	17 ± 2	195 ± 10	3.0 ± 0.2
6	5.2	97.6 ± 0.1	450 ± 20	10.2 ± 0.5	22 ± 2	260 ± 15	4.4 ± 0.2
12	5.3	97.4 ± 0.1	470 ± 20	11.7 ± 0.6	24 ± 2	290 ± 20	4.9 ± 0.2

The mechanical and electrical data are based on the measurements of three samples of each hydrogel. The C/O atomic ratios were calculated according to the peak areas of C and O elements from XPS survey scans, and the C/O atomic ratio of GO precursor is only 2.7.

tween each other. Therefore, the cross-links of the SGH formed by partial overlapping or coalescing of flexible graphene sheets *via* $\pi-\pi$ stacking interactions are much stronger than those of conventional self-assembled hydrogels.

Different from typical chemically cross-linked polymer hydrogels, the SGH behaved like an "elastic-plastic" foam under compression.[38] The compressive stress−strain curve of the SGH showed a linear elasticity at low stresses (regime I) followed by a long plastic regime (regime II) and a densification regime (regime III) over which the stress increased steeply (Figure 3e). There is a sharp drop-point between regimes II and III. We ascribe this phenomenon to partial break of the interior network of the SGH under compression, since the SEM images of the SGH network recorded after this point demonstrated some expanded pores with stretched or even fractured pore walls (Supporting Information, Figure S3). The elastic modulus and yield stress of SGH were measured to be about 0.29 MPa and 24 kPa, respectively, and they are comparable to those of various chemically cross-linked polymer hydrogels.[35]

Self-assembled hydrogels are usually thermally unstable and undergo gel−sol transitions at low temperatures. That is because the weak interactions between their building blocks can be disrupted by thermal stimulation. However, as a distinctive kind of supramolecular hydrogel, our SGH with a strong network is thermally stable, represented by the invariability of its G' and G'' over the entire temperature range of 25−100 °C (Figure 3f). The high thermal stability imparts the SGH another interesting and important property for future applications.

The properties of the SGH strongly depend on GO concentration (C_{GO}) and hydrothermal reaction time. When C_{GO} was low (*e.g.*, 0.5 mg/mL), only a black powdery material was produced after 12 h hydrothermal reduction (Figure 4a), and this result is consistent with that of a previous report.[39] However, as C_{GO} was increased to 1 or 2 mg/mL, mechanically stable SGH samples (SGHs) were obtained. However, the size and strength of the former SGH are smaller than those of the latter. Therefore, we prepared a series of SGHs by hydrothermal reduction of 2 mg/mL GO for different time. The apparent sizes of as-prepared SGHs decreased obviously within the initial 6 h and subsequently changed little (Figure 4b). Besides, all of the SGHs exhibited shear-thinning and viscoelastic behaviors. The mechanical strengths and electrical conductivities of SGHs were increased with reaction time (Table 1). These phenomena can be explained as follows. Before reduction, the GO sheets were randomly dispersed in water and in extended states, due to their strong hydrophilicity and electrostatic repulsion effect.[40] When GO sheets were hydrothermally reduced, they became regionally hydrophobic, due to their restored conjugated domains and diminished oxygenated functionalities as confirmed by the XRD and X-ray photoelectron spectroscopy (XPS) results (Figure 2 and Supporting Information, Figure S2). The combination of hydrophobic and $\pi-\pi$ interactions caused a 3D random stacking between flexible graphene sheets. If C_{GO} was sufficiently high, the cross-linking through partial overlapping of the flexible graphene sheets occurred timely and finally enough cross-linking sites were generated for forming a 3D network with pore sizes ranging from submicrometer to several micrometers (Figure 1c−e).

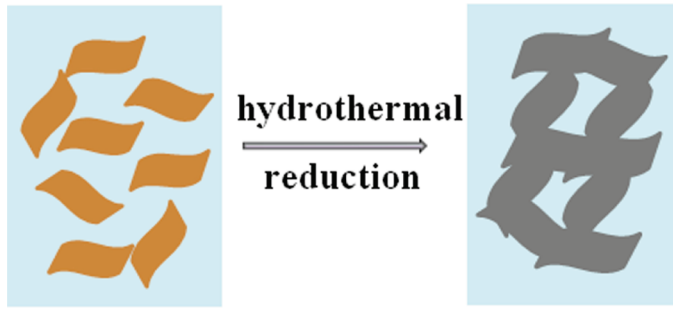

Scheme 1. The proposed formation mechanism for SGH.

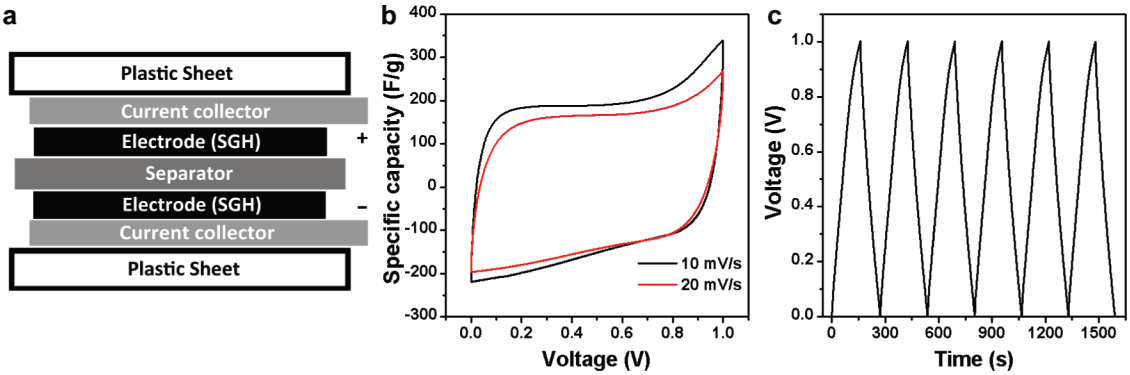

Figure 5. (a) Schematic of SGH-based supercapacitor device; (b) cyclic voltammograms of the SGH-based supercapacitor at two different scan rates; (c) galvanostatic charge/discharge curves of the SGH-based supercapacitor at a constant current of 1 A/g.

Simultaneously, the residual oxygenated functional groups on the graphene sheets could entrap ample water into the graphene network under high temperature and pressure to form a SGH (Scheme 1). With the reaction proceeding, the hydrophobicity and the π-conjugated structures of reduced GO sheets were increased, which enhanced the strength of π−π stacking and increased the amount of cross-links. As a result, the network of SGH became more compact and its water encapsulating ability was weakened (Table 1). However, when C_{GO} was low, the cross-linking would be difficult to occur timely because of the low contacting opportunity between the graphene sheets dispersed in aqueous medium. Consequently, GO sheets were hydrothermally reduced to graphene aggregates and participated as powders.

The SGH can be cut into slices with a knife, and they were used as the electrodes of supercapacitors without using a binding agent and/or conducting additive because of its high porosity and conductivity, and excellent mechanical strength (Figure 5a). The cyclic voltammograms (CV) of the SGH-based supercapacitor are nearly rectangular in shape (Figure 5b), suggesting a good charge transport within the SGH electrodes. The specific capacitances of the SGH at potential scan rates of 10 and 20 mV/s were calculated to be 175 and 152 F/g, respectively, about 50% higher than that of the supercapacitor based on reduced GO agglomerate particles tested under the same condition (100 F/g, scan rate = 20 mV/s),[41] although the SGH-based supercapacitor can be further optimized for its best performance. The high capacitance of SGH was further confirmed by a galvanostatic charge/discharge experiment at a constant current density of 1 A/g (Figure 5c). The specific capacitance of the SGH electrode was evaluated to be about 160 ± 5 F/g (average for 3 capacitors) from the slopes of discharge curves, which is in agreement with CV results.

CONCLUSIONS

We have successfully prepared a mechanically strong, electrically conductive, and thermally stable SGH with high specific capacitance by hydrothermal reduction of GO aqueous dispersion. The method developed here is simple, scalable, and environmental friendly. To the best of our knowledge, the SGH represents the first example of self-assembling 2D graphene sheets into 3D macrostructures *via* a convenient one-step process. Furthermore, there are no similar reports of graphene analogies including carbon nanotubes, fullerenes, and other carbon nanomaterials, demonstrating the uniqueness of graphene. The excellent mechanical, electrical, and thermal properties of the SGH along with the inherent biocompatibility of carbon materials make it attractive in a wide variety of applications, such as drug-delivery, tissue scaffolds, high performance nanocomposites, and supercapacitors. This work provides a deeper understanding of the self-assembly behavior of functionalized graphene as a 2D molecular building block and will inspire more novel designs of hierarchical and functional materials based on graphene.

METHODS

Graphene Oxide (GO) Synthesis and Purification. GO was prepared by oxidation of natural graphite powder (325 mesh, Qingdao Huatai Lubricant Sealing S&T Co. Ltd., Qingdao, China) according to the modified Hummers' method.[42,43] Briefly, graphite (3.0 g) was added to concentrated sulfuric acid (70 mL) under stirring at room temperature, then sodium nitrate (1.5 g) was added, and the mixture was cooled to 0 °C. Under vigorous agitation, potassium permanganate (9.0 g) was added slowly to keep the temperature of the suspension lower than 20 °C. Successively, the reaction system was transferred to a 35−40 °C water bath for about 0.5 h, forming a thick paste. Then, 140 mL of water was added, and the solution was stirred for another 15 min. An additional 500 mL of water was added followed by a slow addition of 20 mL of H_2O_2 (30%), turning the color of the solution from brown to yellow. The mixture was filtered and washed with 1:10 HCl aqueous solution (250 mL) to remove metal ions followed by repeated washing with water and centrifugation to remove the acid. The resulting solid was dispersed in water by ultrasonication for 1 h to make a GO aqueous dispersion (0.5 wt %). The

obtained brown dispersion was then subjected to 30 min of centrifugation at 4000 rpm to remove any aggregates. Finally, it was purified by dialysis for 1 week to remove the remaining salt impurities for the following experiments.

Preparation of Self-Assembled Graphene Hydrogel (SGH). A 10 mL portion of 0.5, 1.0, or 2 mg/mL homogeneous GO aqueous dispersion was sealed in a 16-mL Teflon-lined autoclave and maintained at 180 °C for 1−12 h. Then the autoclave was naturally cooled to room temperature and the as-prepared SGHs were taken out with a tweezer and blotted with a filter paper to remove surface adsorbed water for following experiments. The water content of the SGHs (W_w) was calculated by $W_w = (W_t - W_d)/W_t \times 100$, where W_t is the total weight of the SGH and W_d is the weight of the SGH in the dry state.

Acknowledgment. This work was supported by Natural Science Foundation of China (50873052, 20774056).

Supporting Information Available: Characterization details, additional figures, and discussion. This material is available free of charge *via* the Internet at http://pubs.acs.org.

REFERENCES AND NOTES

1. Novoselov, K. S.; Geim, A. K.; Morozov, S. V.; Jiang, D.; Zhang, Y.; Dubonos, S. V.; Grigorieva, I. V.; Firsov, A. A. Electric Field Effect in Atomically Thin Carbon Films. *Science* **2004**, *306*, 666–669.
2. Geim, A. K. Graphene: Status and Prospects. *Science* **2009**, *324*, 1530–1534.
3. Stankovich, S.; Dikin, D. A.; Dommett, G. H. B.; Kohlhaas, K. M.; Zimney, E. J.; Stach, E. A.; Piner, R. D.; Nguyen, S. T.; Ruoff, R. S. Graphene-Based Composite Materials. *Nature* **2006**, *442*, 282–286.
4. Li, X. L.; Wang, X. R.; Zhang, L.; Lee, S. W.; Dai, H. J. Chemically Derived, Ultrasmooth Graphene Nanoribbon Semiconductors. *Science* **2008**, *319*, 1229–1232.
5. Balandin, A. A.; Ghosh, S.; Bao, W. Z.; Calizo, I.; Teweldebrhan, D.; Miao, F.; Lau, C. N. Superior Thermal Conductivity of Single-Layer Graphene. *Nano Lett.* **2008**, *8*, 902–907.
6. Lee, C.; Wei, X. D.; Kysar, J. W.; Hone, J. Measurement of the Elastic Properties and Intrinsic Strength of Monolayer Graphene. *Science* **2008**, *321*, 385–388.
7. Kim, K. S.; Zhao, Y.; Jang, H.; Lee, S. Y.; Kim, J. M.; Ahn, J. H.; Kim, P.; Choi, J. Y.; Hong, B. H. Large-Scale Pattern Growth of Graphene Films for Stretchable Transparent Electrodes. *Nature* **2009**, *457*, 706–710.
8. Park, S.; Ruoff, R. S. Chemical Methods for the Production of Graphenes. *Nat. Nanotechnol.* **2009**, *4*, 217–224.
9. Gilje, S.; Han, S.; Wang, M.; Wang, K. L.; Kaner, R. B. A Chemical Route to Graphene for Device Applications. *Nano Lett.* **2007**, *7*, 3394–3398.
10. Luo, Z. T.; Lu, Y.; Somers, L. A.; Johnson, A. T. C. High Yield Preparation of Macroscopic Graphene Oxide Membranes. *J. Am. Chem. Soc.* **2009**, *131*, 898–899.
11. Fowler, J. D.; Allen, M. J.; Tung, V. C.; Yang, Y.; Kaner, R. B.; Weiller, B. H. Practical Chemical Sensors from Chemically Derived Graphene. *ACS Nano* **2009**, *3*, 301–306.
12. Lu, C. H.; Yang, H. H.; Zhu, C. L.; Chen, X.; Chen, G. N. A Graphene Platform for Sensing Biomolecules. *Angew. Chem., Int. Ed.* **2009**, *48*, 4785–4787.
13. Shan, C. S.; Yang, H. F.; Song, J. F.; Han, D. X.; Ivaska, A.; Niu, L. Direct Electrochemistry of Glucose Oxidase and Biosensing for Glucose Based on Graphene. *Anal. Chem.* **2009**, *81*, 2378–2382.
14. Wu, Q.; Xu, Y. X.; Yao, Z. Y.; Liu, A. R.; Shi, G. Q. Supercapacitors Based on Flexible Graphene/Polyaniline Nanofiber Composite Films. *ACS Nano* **2010**, *4*, 1963–1970.
15. Zhu, Y. W.; Stoller, M. D.; Cai, W. W.; Velamakanni, A.; Piner, R. D.; Chen, D.; Ruoff, R. S. Exfoliation of Graphite Oxide in Propylene Carbonate and Thermal Reduction of the Resulting Graphene Oxide Platelets. *ACS Nano* **2010**, *4*, 1227–1233.
16. Wang, Y.; Shi, Z. Q.; Huang, Y.; Ma, Y. F.; Wang, C. Y.; Chen, M. M.; Chen, Y. S. Supercapacitor Devices Based on Graphene Materials. *J. Phys. Chem. C* **2009**, *113*, 13103–13107.
17. Xu, Y. X.; Hong, W. J.; Bai, H.; Li, C.; Shi, G. Q. Strong and Ductile Poly(vinyl alcohol)/Graphene Oxide Composite Films with a Layered Structure. *Carbon* **2009**, *47*, 3538–3543.
18. Ramanathan, T.; Abdala, A. A.; Stankovich, S.; Dikin, D. A.; Herrera-Alonso, M.; Piner, R. D.; Adamson, D. H.; Schniepp, H. C.; Chen, X.; Ruoff, R. S.; *et al*. Functionalized Graphene Sheets for Polymer Nanocomposites. *Nat. Nanotechnol.* **2008**, *3*, 327–331.
19. Sun, Z. P.; Hasan, T.; Torrisi, F.; Popa, D.; Privitera, G.; Wang, F. Q.; Bonaccorso, F.; Basko, D. M.; Ferrari, A. C. Graphene Mode-Locked Ultrafast Laser. *ACS Nano* **2010**, *4*, 803–810.
20. Hong, W. J.; Xu, Y. X.; Lu, G. W.; Li, C.; Shi, G. Q. Transparent Graphene/PEDOT-PSS Composite Films as Counter Electrodes of Dye-Sensitized Solar Cells. *Electrochem. Commun.* **2008**, *10*, 1555–1558.
21. Qu, L. T.; Liu, Y.; Baek, J. B.; Dai, L. M. Nitrogen-Doped Graphene as Efficient Metal-Free Electrocatalyst for Oxygen Reduction in Fuel Cells. *ACS Nano* **2010**, *4*, 1321–1326.
22. Si, Y. C.; Samulski, E. T. Exfoliated Graphene Separated by Platinum Nanoparticles. *Chem. Mater.* **2008**, *20*, 6792–6797.
23. Eda, G.; Fanchini, G.; Chhowalla, M. Large-Area Ultrathin Films of Reduced Graphene Oxide as a Transparent and Flexible Electronic Material. *Nat. Nanotechnol.* **2008**, *3*, 270–274.
24. Wang, X.; Zhi, L. J.; Mullen, K. Transparent, Conductive Graphene Electrodes for Dye-Sensitized Solar Cells. *Nano Lett.* **2008**, *8*, 323–327.
25. Hernandez, Y.; Nicolosi, V.; Lotya, M.; Blighe, F. M.; Sun, Z. Y.; De, S.; McGovern, I. T.; Holland, B.; Byrne, M.; Gun'ko, Y. K.; *et al*. High-Yield Production of Graphene by Liquid-Phase Exfoliation of Graphite. *Nat. Nanotechnol.* **2008**, *3*, 563–568.
26. Li, X. L.; Zhang, G. Y.; Bai, X. D.; Sun, X. M.; Wang, X. R.; Wang, E.; Dai, H. J. Highly Conducting Graphene Sheets and Langmuir−Blodgett Films. *Nat. Nanotechnol.* **2008**, *3*, 538–542.
27. Cote, L. J.; Kim, F.; Huang, J. X. Langmuir−Blodgett Assembly of Graphite Oxide Single Layers. *J. Am. Chem. Soc.* **2009**, *131*, 1043–1049.
28. Dikin, D. A.; Stankovich, S.; Zimney, E. J.; Piner, R. D.; Dommett, H. B.; Evmenenko, G.; Nguyen, S. T.; Ruoff, R. S. Preparation and Characterization of Graphene Oxide Paper. *Nature* **2007**, *448*, 457–460.
29. Li, D.; Muller, M. B.; Gilje, S.; Kaner, R. B.; Wallace, G. G. Processable Aqueous Dispersions of Graphene Nanosheets. *Nat. Nanotechnol.* **2008**, *3*, 101–105.
30. Xu, Y. X.; Bai, H.; Lu, G. W.; Li, C.; Shi, G. Q. Flexible Graphene Films *via* the Filtration of Water-Soluble Noncovalent Functionalized Graphene Sheets. *J. Am. Chem. Soc.* **2008**, *130*, 5856–5857.
31. Chen, H.; Muller, M. B.; Gilmore, K. J.; Wallace, G. G.; Li, D. Mechanically Strong, Electrically Conductive, and Biocompatible Graphene Paper. *Adv. Mater.* **2008**, *20*, 3557–3561.
32. Patil, A. J.; Vickery, J. L.; Scott, T. B.; Mann, S. Aqueous Stabilization and Self-Assembly of Graphene Sheets into Layered Bio-nanocomposites using DNA. *Adv. Mater.* **2009**, *21*, 3159–3164.
33. Sangeetha, N. M.; Maitra, U. Supramolecular Gels: Functions and Uses. *Chem. Soc. Rev.* **2005**, *34*, 821–836.
34. Banerjee, S.; Das, R. K.; Maitra, U. Supramolecular Gels 'In Action'. *J. Mater. Chem.* **2009**, *19*, 6649–6687.
35. Calvert, P. Hydrogels for Soft Machines. *Adv. Mater.* **2009**, *21*, 743–756.
36. Murugan, A. V.; Muraliganth, T.; Manthiram, A. Rapid, Facile Microwave-Solvothermal Synthesis of Graphene Nanosheets and Their Polyaniline Nanocomposites for Energy Storage. *Chem. Mater.* **2009**, *21*, 5004–5006.

37. Chen, G. H.; Hoffman, A. S. Graft Copolymers that Exhibit Temperature-Induced Phase Transitions Over a Wide Range of pH. *Nature* **1995**, *373*, 49–52.
38. Lorna, M. F. A.; Gibson, J. *Cellular Solids: Structure and Properties*; Cambridge University Press: Cambridge, 1997; pp 93−98.
39. Zhou, Y.; Bao, Q. L.; Tang, L. A. L.; Zhong, Y. L.; Loh, K. P. Hydrothermal Dehydration for the "Green" Reduction of Exfoliated Graphene Oxide to Graphene and Demonstration of Tunable Optical Limiting Properties. *Chem. Mater.* **2009**, *21*, 2950–2956.
40. Bai, H.; Li, C.; Wang, X. L.; Shi, G. Q. A pH-Sensitive Graphene Oxide Composite Hydrogel. *Chem. Commun.* **2010**, *46*, 2376–2378.
41. Stoller, M. D.; Park, S. J.; Zhu, Y. W.; An, J. H.; Ruoff, R. S. Graphene-Based Ultracapacitors. *Nano Lett.* **2008**, *8*, 3498–3502.
42. Hummers, W. S.; Offeman, R. E. Preparation of Graphitic Oxide. *J. Am. Chem. Soc.* **1958**, *80*, 1339.
43. Xu, Y. X.; Zhao, L.; Bai, H.; Hong, W. J.; Li, C.; Shi, G. Q. Chemically Converted Graphene Induced Molecular Flattening of 5,10,15,20-Tetrakis(1-methyl-4-pyridinio)porphyrin and Its Application for Optical Detection of Cadmium(II) Ions. *J. Am. Chem. Soc.* **2009**, *131*, 13490–13497.